Modeling response spectrum compatible pulse-like ground motion

Guan Chen[a,b], Michael Beer[b,c,d], Yong Liu[a,*]

[a] *State Key Laboratory of Water Resources and Hydropower Engineering Science Institute of Engineering Risk and Disaster Prevention Wuhan University Wuhan 430072 P. R. China.*
[b] *Institute for Risk and Reliability Leibniz Universitt Hannover Hannover 30167 Germany*
[c] *Institute for Risk and Uncertainty and School of Engineering University of Liverpool Liverpool L69 7ZF UK*
[d] *International Joint Research Center for Resilient Infrastructure & International Joint Research Center for Engineering Reliability and Stochastic Mechanics Tongji University Shanghai 200092 P.R. China*

Abstract

The seismic response analysis of near-fault pulse-like ground motions is severely restricted due to the scarcity of pulse-like records. The requirement in regulations that the response spectra of artificial ground motions should be compatible with the target response spectrum makes the relevant studies more difficult. As a result, this study proposes a trigonometric series-based stochastic method to simulate pulse-like ground motions, with the advantage that the corresponding pseudo-spectral acceleration is compatible with the given target response spectrum. This goal is achieved by two parts. (1) The envelope function of pulse-like records obtained by the Hilbert transform is utilized as the amplitude modulation function to ensure that the simulated ground motion contains a pulse. (2) A novel iteration scheme based on random frequency parameters is proposed to guarantee the response spectrum compatibility. The velocity ground motion is first simulated since the pulse usually exists in velocity. The ground-motion acceleration subsequently obtained by differentiating the velocity is adopted to calculate the response spectrum. Two cases are implemented and verified the effectiveness of the proposed method in enriching existing pulse-like databases and generating pulse-like ground motion in areas that lack records. Moreover, the amplitude modulation function and target spectrum, as two key factors in the proposed method, determines the presence of a pulse and the pulse periods, respectively. This property makes the proposed method potentially universal applicability for stochastic pulse-like ground motion simulation in engineering.

Keywords: pulse-like ground motion, near-fault earthquake, response spectrum compatibility,

*corresponding author
Email addresses: guan.chen@irz.uni-hannover.de (Guan Chen), beer@irz.uni-hannover.de (Michael Beer), liuy203@whu.edu.cn (Yong Liu)

ground motion simulation, trigonometric series,

1. Introduction

The near-fault pulse-like ground motion attracts increasing attention since it was reported by Housner and Trifunac [1] and Aki [2] in the 1960s. The findings that the pulse-like ground motion potentially causes severer damage than the ordinary records (e.g., [3, 4, 5]) further advance the relevant studies. However, the scarcity of pulse-like records critically restricts studies that need to consider the randomness of ground motion, e.g., reliability analysis [6, 7]. To mitigate the shortages of records, some ground motion simulation methods were proposed, such as Mavroeidis and Papageorgiou [8] and Dabaghi and Der Kiureghian [9]. However, in accordance with the anti-seismic codes, like Eurocode 8 [10] and ASCE7-16 [11], the response spectrum of artificial ground motion should meet the particular requirements. For example, Eurocode 8 stipulates that no value of the mean 5% damping elastic spectrum should be less than 90% of the corresponding value of the 5% damping elastic response spectrum in the range of periods between $0.2T_1$ and $2T_1$ (T_1 is the fundamental period of the structure in the direction where the accelerogram will be applied). Hence, it is crucial for pulse-like ground motion simulation to contain a pulse in ground-motion velocity and simultaneously compatible with the target spectrum. This study aims to propose a novel stochastic simulation method based on trigonometric series to address this challenge.

The ground motion simulation methods can be briefly grouped into two categories: seismological-based methods and stochastic process-based methods. The former method simulates the ground motions in terms of the seismological mechanism, in which the effects of seismic source mechanism, wave propagation path, and site condition are usually considered (e.g., [12, 13]). The advantages of these methods are that it has clear physical meanings and can effectively analyze the effects of seismic parameters on ground motions. However, accurately determining these seismic parameters is a big challenge. In contrast, the latter treats the ground motions as a stochastic process and focuses on the stochastic property of records. The stochastic technique is widely applied in engineering due to the effectiveness and high efficiency [14]. Hence, the stochastic process-based methods is used in this study to address the limitations of records shortage.

The references investigation for the stochastic processed-based method in pulse-like ground motion simulation was carried out. At the early stage, to efficiently obtain the pulse-like ground motions, the mathematical pulse-like model was proposed based on the statistical characteristics of pulse-like records, like Mavroeidis and Papageorgiou model [8]. Subsequently, various empirical predictive pulse models for different pulse generation mechanisms were proposed, such as the stochastic model for forward-directivity effects [15] and fling-step effects [16]. These methods positively promote the development of seismic response analysis about pulse-like ground motion. However, these mathematical models contain a critical deficiency in that the high-frequency contents are usually ignored. The high-frequency content, on the other hand, is verified to have a significant impact on the structural dynamic response [17]. Hence, to solve the high-frequency issue in mathematical pulse models, the combination strategy by integrating the stochastic non-pulse ground motion and pulse model was proposed. The most common methods for stochastic non-pulse ground motions are the modulated filtered Gaussian white noise model [18] and the Spectral Representation Method (SRM)-based stochastic model [19]. The frequently used pulse models have the Gabor wavelet pulse model [20], the M&P model [8], and the extracted recorded pulse [21]. The feasibility of this strategy was verified, such as the Gabor wavelet pulse model combined with SRM-based non-pulse ground motion [22], the M&P wavelet combined with the modulated filtered white-noise model [9], and the extracted pulse combined with SRM-based non-pulse ground motion [23]. These strategies also effectively solve the high-frequency issue.

However, the response spectrum would dramatically change as the non-pulse ground motion directly adds into the pulse model. Some beneficial efforts on response spectrum compatibility of pulse-like ground motion were made. For example, Zengin and Abrahamson [24] proposed a procedure to modify ground motion to ensure it matches the target response spectrum and instantaneous power spectrum at a specific period interval. Roman-Velez and Montejo [25] collected a large set of pulse-like records as seed to generate ground motions for different magnitude scenarios, and used the continuous wavelet transform-based method to match the narrow-band modified target spectra. Hence, simultaneously ensuring that a high-frequency ground motion contains a pulse and is compatible with the target spectrum is one of the key challenges for pulse-like ground motion simulation.

The response spectrum compatibility methods in ground motion simulation are summarized in Table 1. The amplitude, frequency, and duration are generally regarded as three essential elements of a signal. The effects of ground motion duration on the response spectrum are rarely considered. Hence, we briefly divided the methods into amplitude-, frequency-, and time-frequency-based modification. Thereinto, the time-frequency-based method is mainly related to the wavelet transform since it has great resolutions on both time and frequency domains [26], thus wavelet-based modification used rather than the time-frequency method hereinafter. Besides, other methods like the genetic algorithm [27], which is not related to the stochastic process method, are not discussed in this study. Table 1 shows that the frequency-based modification methods are mainly applied in SRM-based ground motion simulation. Moreover, the frequency is usually modified by the Power Spectral Density Function (PSDF) [28, 29]. The wavelet-based modification is applied widely since it can simultaneously modify the frequency-domain parameters (e.g. response spectrum [30] and power spectra [31, 32]) and time-domain amplitude (e.g. Arias intensity [33]). In contrast, the amplitude-based modification method is used relatively less because it possibly distorts the time-domain attenuation characteristics of ground motion. However, this method is usually more efficient since it directly modifies the time-domain amplitude.

Therefore, based on the trigonometric series, a novel iteration scheme that combines the advantages of both amplitude- and frequency-based modification methods is proposed to simulate response spectrum compatible pulse-like ground motion. Specifically, an amplitude modification function is applied to keep the simulated ground motion containing a pulse and satisfying the attenuation characteristics in the time domain; the frequency parameters are set as the stochastic variables to ensure spectrum compatibility in the frequency domain. The effectiveness of the proposed method in enriching existing pulse-like databases and generating pulse-like ground motions in the areas that lack records is verified by different cases. Furthermore, the ability of compatible with any target spectrum may make the proposed method universal applicability for pulse-like ground motion simulation in engineering.

The organization of this study is constructed as follows: the methodology and the step-by-step procedure for the proposed method are explained in Section 2. Two cases are illustrated in Section 3, which verified that the proposed method is applicable for enriching existing pulse-like records and generating artificial pulse-like ground motions in the area that lacks records. The results and main characteristics of the method are summarized in Section 4. Section 5 investigates the effects of amplitude modulation function and target spectrum on simulated ground motion, together with the differences between the proposed method and SRM on ground motion simulation. The main conclusions are drawn in Section 6.

Table 1: Summary of methods for spectrum compatibility on ground motion simulation

Method	Parameter	Category
$S^{(j+1)}(\omega) = S^{(j)}(\omega)\left[\frac{R^t(\omega)}{R^s_{(j)}(\omega)}\right]$ [28, 34]	$S^{(j)}(\omega)$ is the PSDF at j iteration; $R^t(\omega)$ is the target response spectrum; $R^s_{(j)}(\omega)$ is the response spectrum of simulated ground motion at PSDF=$S^{(j)}(\omega)$.	Frequency-based modification
$S^{(j+1)}(\omega) = S^{(j)}(\omega) + \Delta S^{(j)}(\omega)$ [35]	$\Delta S^{(j)}(\omega)$ is the random PSDF perturbation.	Frequency-based modification
$c^{(n+1)}_{(i,k)}(t) = c^{(n)}_{(i,k)}(t)\frac{R^t(f_i)}{R^s(f_i)}$ [30, 36, 37]	$c^{(n+1)}_{(i,k)}(t)$ is the wavelet decomposed coefficients as the scale and location parameters are i and k, respectively; $R^t(f_i)$ is the target response spectrum at frequency range f_i ; and $R^s(f_i)$ is the response spectrum of $c^{(n)}_{(i,k)}(t)$.	Wavelet-based method
$w^{(n+1)}(i,k) = \frac{R^t(f_i)}{R^s(y^{(n)}(t),f_i)}$ [33, 37]	$w^{(n+1)}(i,k)$ is the wavelet packet coefficients, $R^t(f_i)$ is the target response spectrum of frequency range f_i , and $R^s(y^{(n)}(t), f_i)$ is the response spectrum of $w^{(n)}(i,k)$.	Wavelet-based method
$f^{(n+1)}(t) = f^{(n)}(t) + \alpha^{(n)}\widetilde{f}^{(n)}(t)$ [38]	$f^{(n)}(t)$ is the reconstruction results of wavelet transform, α is the correction factor, $\widetilde{f}^{(n)}(t)$ time-frequency jointly-localized component.	Wavelet-based method
$a^{(n+1)}_g(t) = a^{(n)}_g(t) + \Delta a_g(t)$ [39, 40]	$a^{(n)}_g(t)$ is simulated ground motion in different iteration; the selection of $\Delta a_g(t)$ is defined as a L_∞ norm optimization problem.	Amplitude-based modification

2. Methodology

2.1. Pseudo-acceleration response spectrum

For the linear single-degree of freedom (SDOF) system, the dynamic response subjected to seismic excitation is expressed as Eq. (1).

$$m\ddot{u}_r + c\dot{u}_r + ku_r = -m\ddot{u} \tag{1}$$

where m is the mass; c is the viscous damping coefficient; k is the stiffness; u_r , $\dot{u}_r$ and $\ddot{u}_r$ are relative response displacement, velocity and acceleration, respectively; and $\ddot{u}$ is the excitation acceleration of seismic ground motion.

Using damping ratio ξ and natural angular frequency ω_n of non-damping system, Eq. (1) is rewritten in Eq. (2).

$$\ddot{u}_r + 2\xi\omega_n\dot{u}_r + \omega_n^2 u_r = -\ddot{u} \tag{2}$$

where damping ratio $\xi = c/(2m\omega) = c/(2\sqrt{mk})$; and natural angular frequency $\omega_n = \sqrt{k/m} = 2\pi/T$.

Based on Duhamel's integral, the solution of Eq. (2) is expressed in Eq. (3).

$$u_r(t) = \ddot{u}(t) * h(t) = \int_0^t \ddot{u}(\tau)h(t-\tau)\mathrm{d}\tau \tag{3}$$

$$h(t) = -\frac{1}{\omega_d}e^{-\xi\omega_n t}\sin(\omega_d t) \tag{4}$$

where $*$ means convolution calculation; $h(t)$, for $t > 0$, is the impulse response function; ω_d is the damped natural frequency, $\omega_d = \sqrt{1-\xi^2}\omega_n$.

The maximum displacement values ($max\,|u_r|$) under the different natural frequencies ω_n with certain damping ratio ξ are the displacement response spectrum $S_d(\xi, \omega_n)$, as shown in Eq. (5).

$$S_d(\xi, \omega_n) = \max|u_r(t)| \tag{5}$$

The pseudo-velocity response spectrum $S_v(\xi, \omega_n)$ and pseudo-acceleration response spectrum $S_a(\xi, \omega_n)$ of ground motion are defined in Eqs. (6) and (7), respectively.

$$S_v(\xi, \omega_n) = \omega_n \max|u_r(t)| \tag{6}$$

$$S_a(\xi, \omega_n) = \omega_n^2 \max|u_r(t)| \tag{7}$$

2.2. Trigonometric series-based ground motion velocity

The trigonometric series is a feasible and efficient form in generating non-stationary Gaussian processes (e.g., [19, 41, 42]). Thus, this form is also adopted in the proposed method to simulate pulse-like ground motions. Compared with the classical SRM, the proposed method does not concern the PSDF, but directly synthesize the ground motion in the time domain using the trigonometric series. The differences between the proposed method and SRM are elaborated in Section 5.2. Besides, the ground-motion velocity is initially generated in this study instead of acceleration that other methods usually adopt since the pulse usually exists in the velocity. The ground-motion acceleration subsequently obtained by differentiating the velocity is adopted to calculate the response spectrum.

In mathematics, a series with form in Eq. (8) is called trigonometric series.

$$F_n(x) = \frac{A_0}{2} + \sum_{n=1}^{\infty}(A_n \cos nx + B_n \sin nx) \tag{8}$$

Based on Eq. (8), a trigonometric series-based form for ground-motion velocity $\dot{u}(t)$ is proposed, as shown in Eq. (9).

$$\dot{u}(t) = \sum_{i=1}^{n} \dot{u}_i(t) = \sum_{i=1}^{n} A(t)\cos(\omega_i t + \phi_i) \tag{9}$$

where $\dot{u}_i(t)$ is the component of the ground-motion velocity; $A(t)$ is the amplitude modulation function, which is fixed in this study to make the simulated ground-motion velocity containing a pulse; t is the time series of ground motions; ω_i is a frequency variable in the interval of $[0, \omega_s]$, in which ω_s is the half of sampling frequency of recorded ground motions; and ϕ_i is a phase variable in the interval of $[0, 2\pi]$. In accordance with the central limit theorem, the simulated ground motion $\dot{u}(t)$ obeys Gaussian random process when n tends to positive infinity.

Inputting the differential of Eq. (9) into Eq. (3), the response displacement under seismic excitation is expressed in Eq. (10).

$$u_r(t) = \int_0^t \sum_{i=1}^{n} \ddot{u}_i(\tau) h(t-\tau) \mathrm{d}\tau \tag{10}$$

where the acceleration $\ddot{u}_i(t)$ is the differential of the i^{th} velocity component $\dot{u}_i(t)$, and $\ddot{u}_i(t) = d\dot{u}_i(t)/dt = d(A(t)\cos(\omega_i t + \phi_i))/dt$.

In accordance with the additivity of integration, Eq. (10) is rewritten to Eq. (11).

$$u_r(t) = \sum_{i=1}^{n} \int_0^t \ddot{u}_i(\tau) h(t-\tau) \mathrm{d}\tau = \sum_{i=1}^{n} u_{r,i}(t) \tag{11}$$

where $u_{r,i}(t)$ is the response displacement of the i^{th} trigonometric series-based acceleration component $\ddot{u}_i(t)$. It indicates that the final response displacement of ground motion can be expressed by the sum of sub-response displacement of the ground motion components.

Since the pseudo-acceleration response spectrum is based on the response displacement as shown in Eq. (7), the pseudo-acceleration response spectrum of ground motion is expressed in Eq. (12).

$$S_a(\xi, \omega_n) = \omega_n^2 \max\left|\sum_{i=1}^{n} u_{r,i}(t)\right| \tag{12}$$

Hence, the pseudo-spectral acceleration of ground motion also depends on the sub-response spectrum of components. Based on this property, an iteration scheme for simulating response spectrum compatible pulse-like ground motions is proposed.

2.3. Iteration scheme for response spectrum compatible pulse-like ground motion

To evaluate the compatibility between pseudo-spectral acceleration of simulated ground motion $S_a^s(T)$ and target spectrum $S_a^t(T)$, the error ϵ used in Shields [35] is adopted, as shown in Eq. (13).

$$\epsilon = \sqrt{\frac{\sum_{k=0}^{N-1}[S_a^t(T_k) - S_a^s(T_k)]^2}{\sum_{k=0}^{N-1}[S_a^t(T_k)]^2}} \tag{13}$$

where $S_a^t(T_k)$ is the target response spectrum; $S_a^s(T_k)$ is the elastic pseudo-acceleration response spectrum of the simulated ground motion; and T_k is the corresponding period of response spectrum.

Based on Eqs. (12) and (13), the variables on the response spectrum-compatible pulse-like ground motion simulation include trigonometric series-based ground motion velocity $\dot{u}(t)$, damping ratio ξ, response spectrum error ϵ and target response spectrum $S_a^t(T)$. Among them, the value of ξ and ϵ is generally stipulated in the anti-seismic codes. For example, Eurocode 8 recommends damping ratio ξ is 5%, and the spectrum error ϵ at the particular period range should be less than 10%. The target response spectrum $S_a^t(T)$ depends on the research purpose. The site conditions-based designed response spectrum in anti-seismic codes is often applied as the target spectrum to generate ground motions. Hence, after these three variables are determined, the trigonometric series-based ground motion velocity $\dot{u}(t)$ is the only parameter that can be utilized to generate response spectrum compatible pulse-like ground motion.

The trigonometric series-based ground motion velocity $\dot{u}(t)$ (see Eq. (9)) depends on the amplitude modulation function $A(t)$ and frequency-domain parameters ω and ϕ_i in this study. To ensure the response spectrum compatibility and the presence of a pulse, We use the amplitude modulation function $A(t)$ to govern the time-domain characteristics of simulated ground motion, and frequency variable ω_i and phase variable ϕ_i to control the pseudo-spectral acceleration of ground motion. Specifically, $A(t)$ is fixed to enable the simulated ground motion to contain a pulse. The frequency variable ω_i and phase variable ϕ_i are set as random variables in an iteration scheme to ensure response spectrum compatibility.

Therefore, the amplitude modulation function and the iteration scheme are two key issues in modeling response spectrum compatible pulse-like ground motion. The Hilbert transform is validated as a workable tool to extract time-domain characteristics of ground motion [43]. Hence, the envelope function of pulse-like records obtained by the Hilbert Transform is regarded as the amplitude modulation function. Because the ground-motion velocity is first simulated in this study (see Eq. (9)), the amplitude modulation function is also the envelope function of velocity records.

The principle for Hilbert transform obtaining envelope function is introduced herein. For a signal $x(t)$, the analytic signal $\zeta(t)$ is defined in Eq. (14) based on Hilbert transform [44].

$$\zeta(t) = x(t) + j\tilde{x}(t) \tag{14}$$

$$\tilde{x}(t) = x(t) * \frac{1}{\pi t} = \frac{1}{\pi} \int_{-\infty}^{+\infty} \frac{x(\tau)}{t-\tau} \mathrm{d}\tau \tag{15}$$

where $j = \sqrt{-1}$; $*$ presents convolution; $\tilde{x}(t)$ is the Hilbert transform of $x(t)$.

The envelope function $f_e(t)$ of $x(t)$ is obtained by Eq. (16).

$$f_e(t) = \sqrt{x^2(t) + \tilde{x}^2(t)} \tag{16}$$

More details about Hilbert transform in obtaining envelope function can be found in Feldman [45]. Besides, although the envelope function determines the shape of the amplitude modulation function, the maximum value of the envelope function can affect the convergence of the iteration scheme. It is because each component needs to be modulated to ensure the presence of a pulse in the proposed method rather than only finally modulating the stochastic process to enable ground motion to meet the time-domain attenuation characteristics. The optimum maximum value of the envelope function is recommended in Section 5.1 based on tests.

On the other hand, to guarantee the response spectrum compatibility, a novel iteration scheme is proposed based on the pseudo-spectral acceleration relationship between the ground motion and the components (see Eq. (12)). The core idea of the iteration scheme is using random trigonometric series that fixes the envelope but varies the frequency parameters to synthesize response spectrum compatible pulse-like ground motion in the time domain. A step-by-step procedure of the iteration scheme is explained in the next section.

2.4. Step-by-step procedure

The step-by-step flowchart of the proposed algorithm is shown in Figure 1. The details are elaborated as follows.

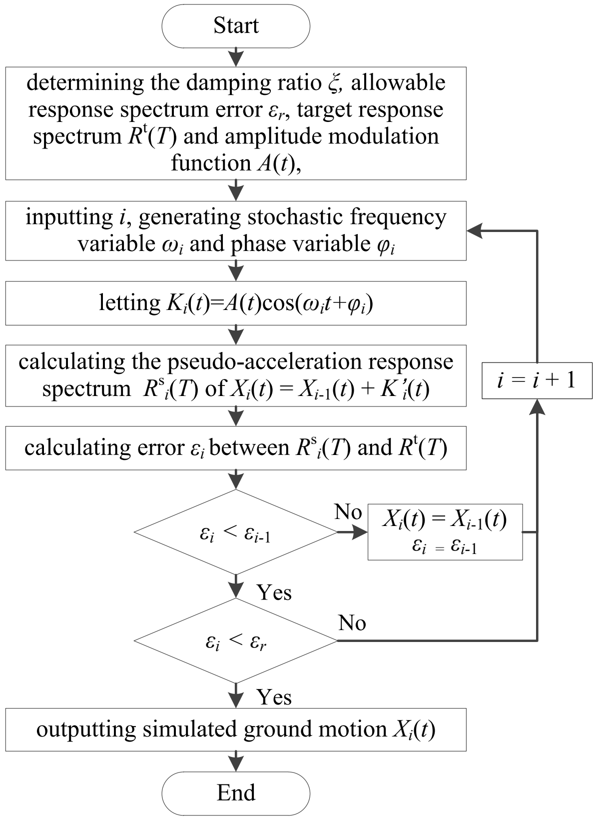

Figure 1: Flowchart of the proposed algorithm.

Initially, the damping ratio ξ, response spectrum error ϵ_r, target response spectrum $S_a^t(T)$ and the amplitude modulation function $A(t)$ need to be determined. The value of ξ and ϵ_r is particularly stipulated in the anti-seismic codes, and generally set to 5% and 10%, respectively. The target response spectrum $S_a^t(T)$ is based on the research purpose. Any target spectrum is feasible for the proposed method theoretically. As explained in Section 2.3, the envelope function of pulse-like records obtained by the Hilbert transform is adopted as the amplitude modulation function $A(t)$.

Subsequently, the iteration scheme is performed based on the stochastic frequency-domain parameters ω_i and ϕ_i in Eq. (9). The main iteration equation is $X_i = X_{i-1} + K_i'$, where $X_0 = 0$ and $K_i = A(t)\cos(\omega_i t + \phi_i)$. For each $X_i(t)$, the pseudo-spectral acceleration $S_{a,i}^s(T)$ is calculated based on Eq. (7). Then, the spectrum error ϵ_i between the $S_{a,i}^s(T)$ and target spectrum $S_a^t(T)$ is calculated based on Eq. (13).

Finally, the error ϵ_i and ϵ_{i-1} is compared. The component K_i would be accepted if the ϵ_i becomes less. Otherwise, the above steps are repeated. The iteration is terminated as the ϵ_i less than ϵ_r. The final $X_i(t)$ is the simulated ground motion.

3. Case study

Two cases are illustrated in this section. Case 1 aims at enriching the pulse-like ground motions based on the existing records. Hence, the algorithm parameters in this case are based on pulse-like records. Case 2 aims to generate ground motions in the areas that lack records. In this situation, we generate the pulse-like ground motions based on the target response spectrum and a designed amplitude modulation function.

3.1. Case 1: Using recorded pulse-like ground motion

A typical recorded pulse-like velocity ground motion on Imperial Valley-06 Earthquake from Pacific Earthquake Engineering Research Center (PEER) Ground Motion Database is selected in this case (i.e., the horizontal 1 direction of record sequence number 185 in PEER NGA-West2 flatfile). The ground-motion velocity, acceleration, pseudo-spectral velocity (S_v), and pseudo-spectral acceleration (S_a) of selected pulse-like ground motion with 5% damping ratio are shown in Figure 2(a), (b), (c), and (d), respectively.

Besides, as one of the most significant parameters, the pulse period (T_p) of the selected ground motion is identified based on the identification method in Chen et al. [46]. This method is based on the convolution analysis, which is theoretically consistent with the continuous wavelet transform-based method in Baker [21], but overcomes the limitation of wavelet transform that requires a wavelet basis [47]. Based on the identification method, the pulse part is extracted, as shown in Figure 2(a). The pseudo-spectral velocity of the pulse part and residual ground motion is also included in Figure 2(c).

Following the procedures in Figure 1, the damping ratio ξ, allowable error ϵ_r, the target response spectrum $S_a^t(T)$ and amplitude modulation function $A(t)$ need to be fixed before performing the iteration scheme. The damping ratio is set to 5%, and the error is set to 10% based on the stipulation in Eurocode 8 that the error between the target response spectrum and the pseudo-acceleration response spectrum of simulated ground motion should be less 10%. The pseudo-spectral acceleration of the selected pulse record (see Figure 2 (d)) is regarded as the target response spectrum. The envelope function of selected velocity records obtained by Hilbert transform is regarded as amplitude modulation function, as shown in Figure 3. Besides, the maximum

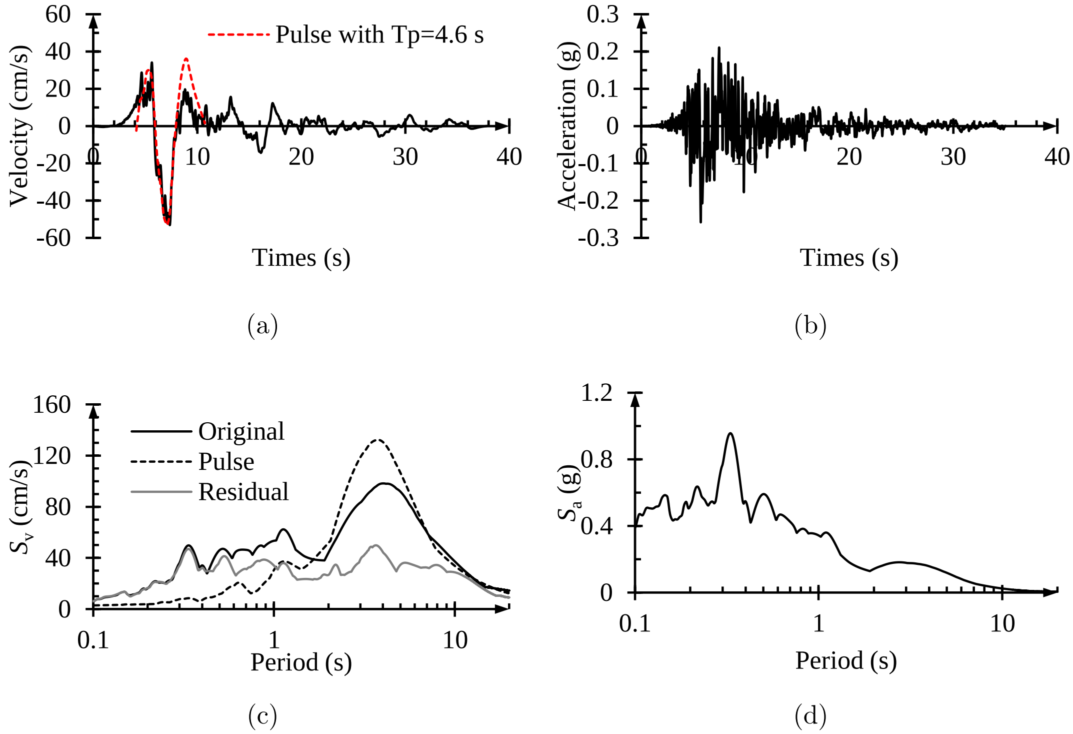

Figure 2: (a) Velocity, (b) acceleration, (c) pseudo-spectral velocity (S_v) and (d) pseudo-spectral acceleration (S_a) of selected pulse-like ground motion in Imperial Valley-06 Earthquake.

value of the amplitude modulation function is scaled to 0.5 to ensure that the iteration scheme can quickly converge to the allowable error.

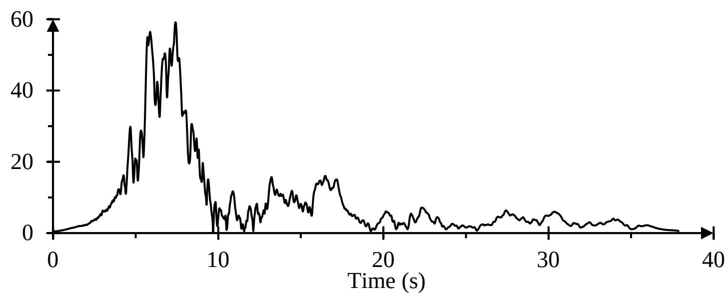

Figure 3: Envelope function of selected velocity records in Figure 2(a) obtained by Hilbert transform. The scaled envelope function is the amplitude modulation function of Case 1.

After the parameters are determined, the iteration scheme is carried out to obtain response spectrum compatible pulse-like ground motions. An example for simulated ground-motion velocity, acceleration, pseudo-spectral velocity, and pseudo-spectral acceleration is plotted in Figure 4. The pulse period and the pseudo-spectral velocity of the pulse part and residual ground motion are also included. It shows that simulated ground-motion velocity contains an obvious pulse. Moreover, the pseudo-spectral acceleration of simulated ground motion simultaneously agrees with the target spectrum. Hence, the proposed method can effectively enrich the pulse-like databases by using the envelope function and pseudo-spectral acceleration of pulse-like records.

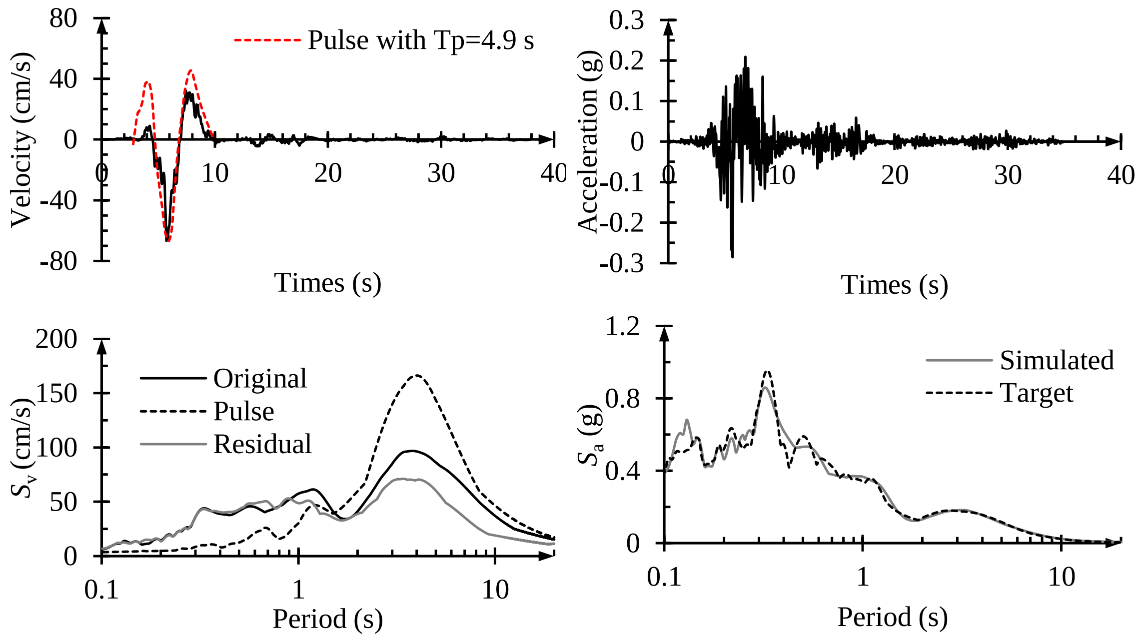

Figure 4: Case 1: Using recorded pulse-like ground motion. An example for simulated ground-motion velocity, acceleration, pseudo-spectral velocity (S_v), and pseudo-spectral acceleration (S_a) with 5% damping ratio. The spectrum error defined in Eq. (13) is 10%.

3.2. Case 2: Using target response spectrum

For the areas that lack ground-motion records, it is usually required to generate artificial ground motions based on the target response spectrum. This issue is addressed in Case 2. Specifically, the target response spectrum in anti-seismic codes and a designed amplitude modulation function are adopted to simulate the response spectrum compatible pulse-like ground motion.

The parameters in Case 2 are set as follows. The damping ratio is set to 5%. The allowable error between the target response spectrum and the pseudo-spectral acceleration of simulated ground motion is set to 5% to test the robustness of the proposed algorithm. The designed 5% damping horizontal response spectrum defined in Eurocode 8 for Spectra Type 1 and Ground

Type C is employed as the target spectrum. It is expressed in Eq. (17), and plotted in Figure 5.

$$S_a^t(T) = \begin{cases} a_g \cdot S(1+1.5T/T_B), & (0 \leqslant T \leqslant T_B) \\ 2.5a_g \cdot S, & (T_B \leqslant T \leqslant T_C) \\ 2.5a_g \cdot S \cdot T_C/T, & (T_C \leqslant T \leqslant T_D) \\ 2.5a_g \cdot S \cdot T_C \cdot T_D/T^2, & (T_D \leqslant T \leqslant 6) \end{cases} \tag{17}$$

where $S_a^t(T)$ is the target response spectrum; T is the vibration period of a linear single-degree of freedom system; and a_g is the designed ground motion acceleration, which is set to 0.28; The ground type parameters $S = 1.15$, $T_B = 0.2$ s, $T_C = 0.6$ s, and $T_D = 2.0$ s.

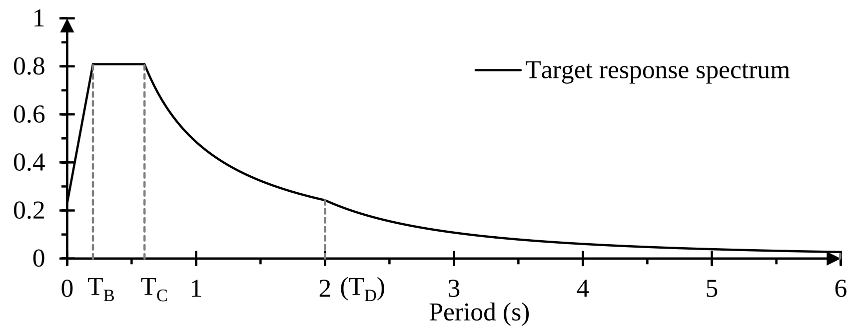

Figure 5: The target response spectrum defined in Eurocode 8 for Spectra Type 1 and Ground Type C.

The pulse-like ground motions of Imperial Valley-06 Earthquake, which are identified in Baker's study [21], are utilized to design the amplitude modulation function. Initially, the envelope functions of pulse-like records are obtained based on Hilbert Transform. Subsequently, the mean value of envelope functions is calculated. Finally, referring to the form of amplitude modulation function in Jennings et al. [48], a piecewise function is proposed to fit the mean value. The envelope function of each pulse-like record, mean value, and the fitting function are plotted in Figure 6. The piecewise function is expressed in Eq. (18). This equation is the designed amplitude modulation function for Case 2. The maximum value of the amplitude modulation function is also scaled to 0.5 before the iteration. The duration of simulated ground motion is set to 35 s.

$$A(t) = \begin{cases} t^3/125 & (0 \leqslant t \leqslant 5) \\ 1 & (5 \leqslant t \leqslant 7.5) \\ 4.913e^{-0.2121t} & (7.5 \leqslant t \leqslant 15) \\ 0.335 - 0.009t & (15 \leqslant t \leqslant 35) \end{cases} \tag{18}$$

Based on the determined parameters above, the iteration scheme defined in Figure 1 is carried out. An example for simulated ground-motion velocity, acceleration, pseudo-spectral velocity, and

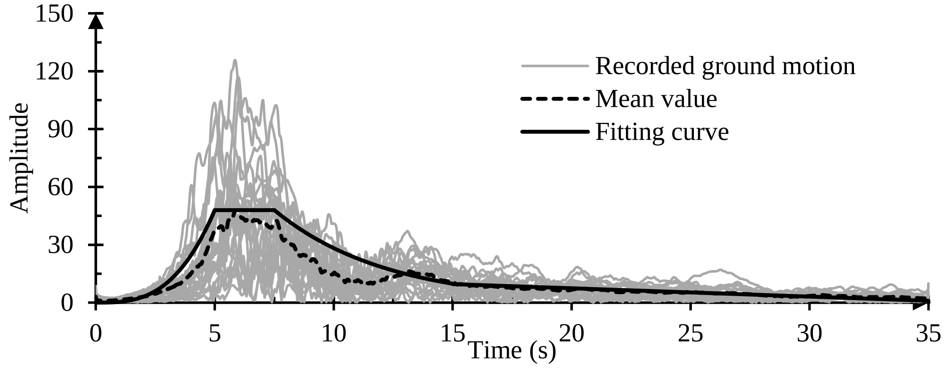

Figure 6: Mean value and fitting curve for envelope functions of pulse-like records in Imperial Valley-06 Earthquake. The grey line is the envelope function of each pulse-like record obtained by the Hilbert transform. The fitting curve is the designed amplitude modulation function in Case 2.

pseudo-spectral acceleration is plotted in Figure 7. The pulse period and the pseudo-spectral acceleration of the pulse part and residual ground motion are also included. It shows that the simulated ground-motion velocity contains an obvious pulse. Moreover, the pseudo-spectral acceleration of simulated ground motion is compatible with the target response spectrum.

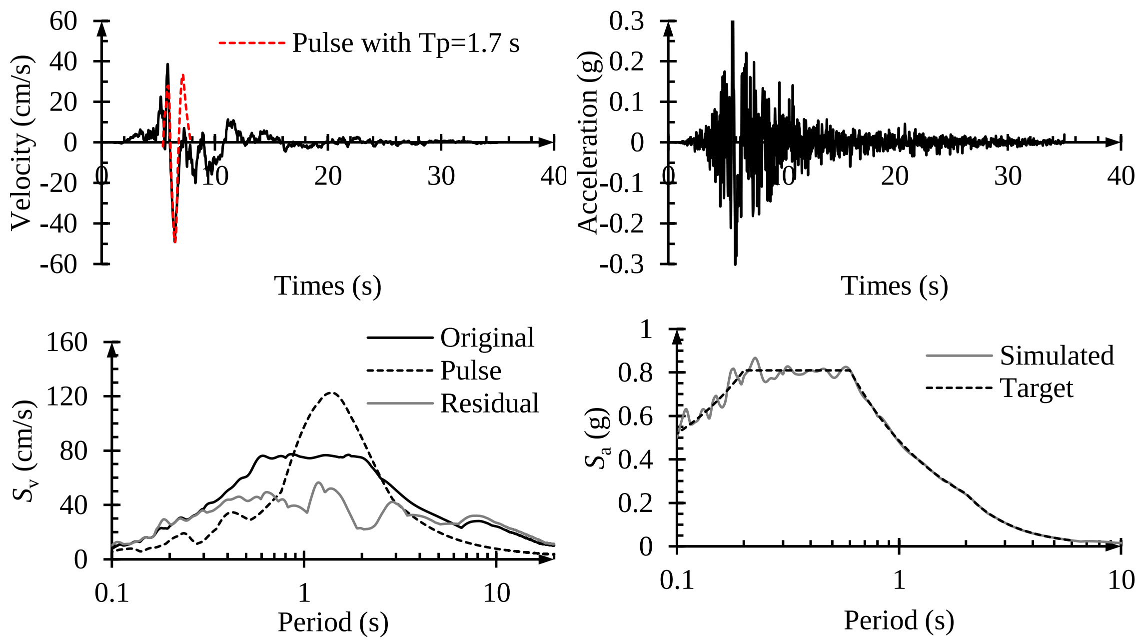

Figure 7: Case 2: Using target response spectrum. An example for simulated ground-motion velocity, acceleration, pseudo-spectral velocity (S_v), and pseudo-spectral acceleration (S_a) with 5% damping ratio. The spectrum error defined in Eq. (13) is 5%.

Combining Figures 4 and 7 shows that the pulse period in Case 2 differs from Case 1. Hence, the pulse characteristics can vary by adopting different amplitude modulation functions and target spectra. It means that the proposed method can simulate diverse response spectrum compatible pulse-like ground motions. In addition, since both cases contain an obvious pulse, the envelope function of pulse-like records obtained by Hilbert transform and the designed piecewise function (see Eq. (18)) are workable amplitude modulation functions in simulating pulse-like ground motion.

4. Results

The effectiveness of the proposed method in simulating response spectrum compatible pulse-like ground motion was verified by two cases. It indicates that the proposed method can not only enrich the pulse-like databases but also generate the artificial pulse-like ground motions based on the target response spectrum and the designed amplitude modulation function. Moreover, the pseudo-spectral acceleration of simulated pulse-like ground motions can simultaneously be compatible with the target response spectrum.

Besides the advantage of the response spectrum compatibility, other characteristics of the proposed method in pulse-like ground motion simulation are also highlighted herein. (1) The simulated pulse-like velocity obeys the Gaussian random process. This property ensures that the simulated ground motions agree with the Gaussian process assumption that the stochastic methods generally adopted. (2) The proposed iteration scheme possesses great robustness property in spectrum compatibility analysis. The pseudo-spectral acceleration of simulated ground motion can precisely match the target spectrum that contains a large data amount. For example, although the target spectrum in the cases uses 200 Hz frequency sampling to 6 s (i.e., 1200 data points), the pseudo-spectral acceleration of simulated ground motion can be compatible with the target spectrum at the required error value. (3) Since both the envelope function of pulse-like records obtained by Hilbert transform and the designed piecewise function are feasible amplitude modulation functions, the pulse characteristics of simulated pulse-like ground motion can be various. It ensures the diversity of simulated ground motions.

5. Discussion

5.1. Effects of amplitude modulation function and target spectrum

In practice, because the damping ratio ξ, response spectrum error ϵ_r, together with the random frequency parameters in the iteration scheme are usually unchangeable for the proposed method, the target response spectrum $S_a^t(T)$ and the amplitude modulation function $A(t)$ are two key variables for simulated ground motion. Hence, to determine the specific influences of these two factors on ground motion, four types of response spectrum-compatible pulse-like ground motions are simulated based on two amplitude modulation functions and three target spectra. The recorded and designed amplitude modulation function (see Figure 8(a)) is the envelope function of selected ground motion (see Figure 3) and the fitting curve defined in Eq. (18) (see Figure 6). The Eurocode8, designed and recorded target spectra (see Figure 8(b)) are the spectrum defined in Eurocode 8 (see Figure 5), the average spectral acceleration of the pulse-like ground motions in Imperial Valley-06 Earthquake, and spectral acceleration of selected ground motion (see Figure 2(d)), respectively. The maximum value of and the value at 0 s of three target spectra are modified to be consistent to minimize the effects of variables. Besides, the damping ratio ξ and spectrum error ϵ are set to 5% and 10%, respectively.

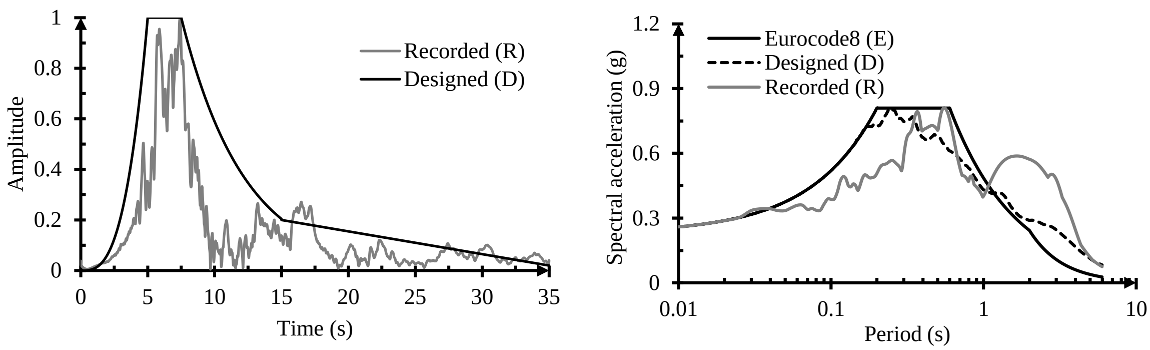

(a) (b)

Figure 8: (a) Amplitude modulation functions and (b) target spectra adopted in response spectrum-compatible pulse-like ground motion simulation.

Examples for the four types of pulse-like ground motions (named D-E, R-E, R-D, and R-R ground motion) are plotted in Figure 9 (a), (b), (c) and (d), respectively. Specifically, D-E ground motion adopts the designed amplitude modulation function and Eurocode8 target spectrum; R-E ground motion adopts the recorded amplitude modulation function and Eurocode8 target spectrum; R-D adopts the recorded amplitude modulation function and designed target spectrum, and R-R ground motion adopts the recorded amplitude modulation function and recorded target spectrum. Two hundred ground motions are simulated for each type due to the stochastic properties of the simulation procedure. The pulse period of the simulated ground motion is also identified, as shown in Figure 10.

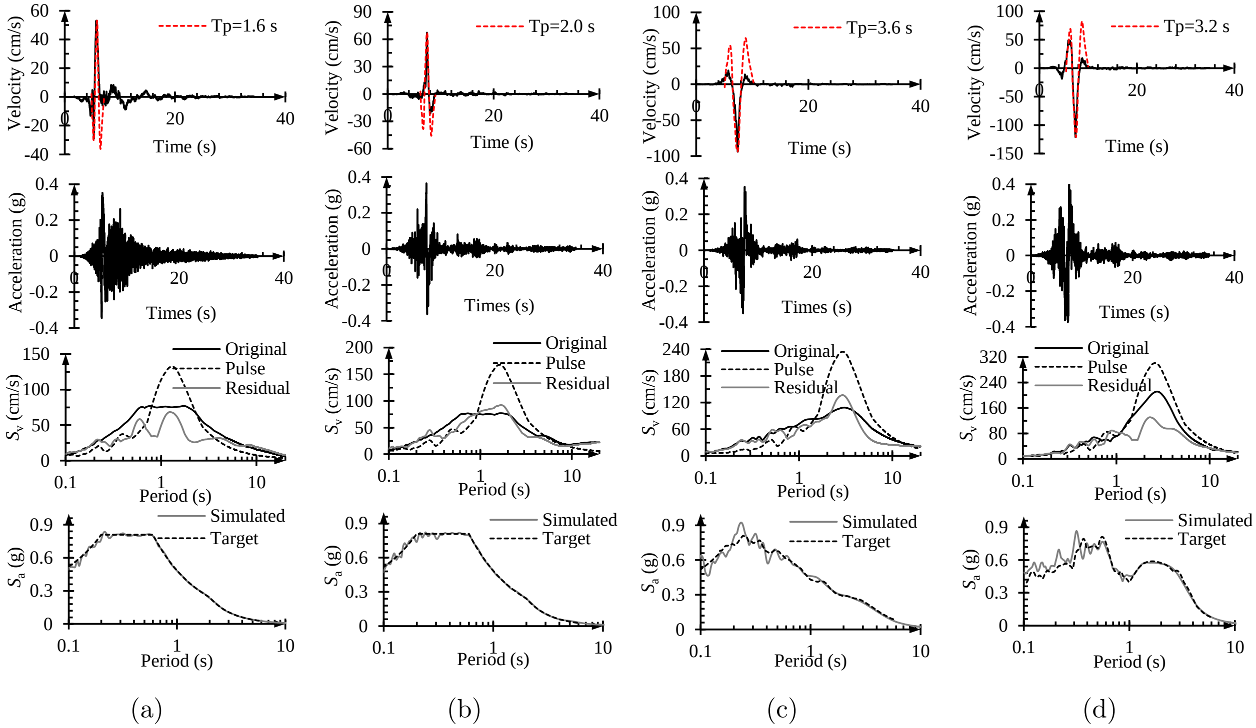

Figure 9: Velocity, acceleration, pseudo-spectral velocity and acceleration of (a) D-E, (b) R-E, (c)R-D, and (d)R-R ground motion. The damping ratio is 5%, and the spectrum error defined in Eq. (13) is 10%.

Figure 9 shows that the simulated ground motion can contain a pulse in velocity and simultaneously be compatible with the given target spectrum. Moreover, the compatibility of three different target spectra indicates that the proposed method can generate pulse-like ground motion compatible with any target spectrum. The applicability of different amplitude modulation functions ensures that the pulse characteristics of simulated pulse-like ground motions can be diverse. Hence, the proposed method is potentially a universally applicable stochastic method for pulse-like ground motion simulation.

Figure 10 indicates that the presence of a pulse in ground motion depends on the amplitude modulation function; however, the pulse period is more related to the target spectra. For example, D-E and R-E ground motions, which adopt the same target spectrum but different amplitude modulation functions, have similar pulse periods. In contrast, the pulse periods of R-E, R-D, and R-R ground motions vary while they adopt the same amplitude modulation function but different target spectra.

Besides, the maximum value of the amplitude modulation function can affect the convergence of the proposed iteration scheme. To determine the optimum maximum value of amplitude mod-

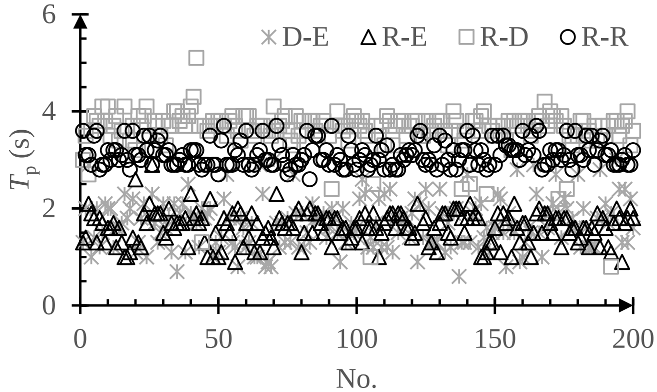

Figure 10: Pulse period comparison of four types of simulated ground motion. The average pulse period of D-E, R-E, R-D and R-R ground motion is 1.7 s, 1.6 s, 3.6 s, and 3.1 s, respectively.

ulation function, the recorded amplitude modulation function and Eurocode8 are selected as the amplitude modulation function and the target response spectrum to perform the iteration scheme in Figure 1, respectively. Six different maximum values are tested, including 0.01, 0.1, 0.5, 1, 10 and 100. 50,000-time iteration is carried out for each value. Moreover, the average of 10-time calculations is adopted as the final convergence result to reduce the randomness error. The relationship between iteration time and response spectrum error is shown in Figure 11. It indicates that the iteration scheme does not converge to the allowable error when the amplitude value is larger than 10. In contrast, the iteration scheme converges with quite low speed when the amplitude value is smaller than 0.01. Therefore, based on the tests, the optimum maximum value of the amplitude modulation function is $[1/100, 1/50]$ of target peak ground velocity.

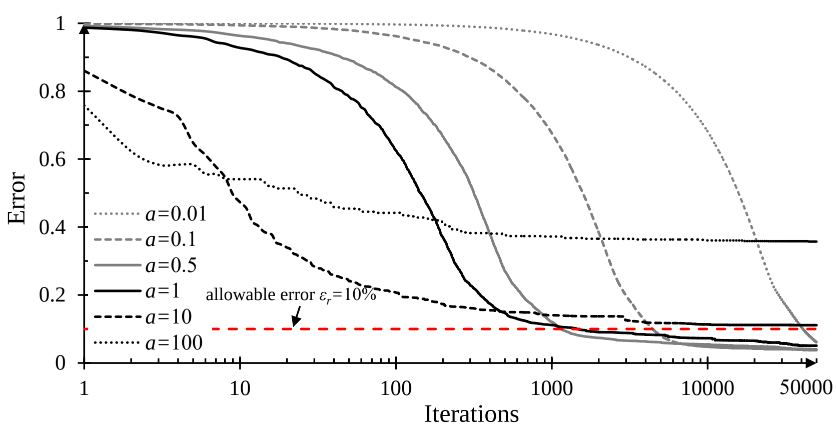

Figure 11: Effects of maximum value (a) of amplitude modulation function on convergence of iteration scheme. Each curve is based on the average of 10-time calculations.

5.2. Comparison with spectral representation method

Spectral representation method (SRM), as an effective way in stochastic process simulation, is widely applied in ground motion simulation (e.g.,[19, 28]) since it was proposed by Shinozuka and co-workers [49, 50, 51]. A Gaussian random process $Y_n(t)$ with zero-mean, unit-variance can be expressed in Eq. (19) in accordance with SRM.

$$Y_n(t) = \sum_{k=1}^{n} \sqrt{2}\sigma_k \cos(\omega_k t + \phi_k) \tag{19}$$

where ω_k and t are the frequency and time parameters, respectively; ϕ_k are the uniform variables in the interval $[0, 2\pi]$; and σ_k satisfies Eq. (20).

$$\sigma_k^2 = \int_{\omega_k-\Delta\omega/2}^{\omega_k+\Delta\omega/2} G(\omega)\mathrm{d}\omega \approx G(\omega_k)\Delta\omega \tag{20}$$

where $G(\omega)$ is the one-side Power Spectral Density Function (PSDF); $\Delta\omega = \omega_0/n$ and $\omega_k = (k-1/2)\Delta\omega$. ω_0 is the truncation frequency of the $G(\omega)$, beyond which $G(\omega)$ is assumed to be zero [52].

A time-domain modulation procedure needs to perform to ensure that the generated Gaussian random process satisfies the time-domain attenuation characteristics of seismic ground motions. The time-domain modulation expression is shown in Eq. (21).

$$G_n(t) = f(t)Y_n(t) \tag{21}$$

where $f(t)$ is the amplitude modulation function. $G_n(t)$ is the simulated ground motion.

A typical ground motion (see Figure 12) is generated based on SRM. The PSDF of the recorded pulse-like velocity ground motion in Figure 2 is adopted in the simulation. Figure 12 shows that its pulse characteristic is unapparent. Furthermore, the response spectrum of the simulated ground motion is not compatible with the target response spectrum.

As mentioned in Table 1, some researches have been carried out for the response spectrum compatibility in SRM-based ground motion simulation, such as the classical iteration scheme based on the PSDF [28] and the perturbation algorithm proposed by Shields [35]. The expression of the classical iteration scheme is shown in Eq. (22). The feasibility of this iteration scheme in acceleration ground motion simulation is widely verified [34]. However, two challenges exist for this scheme in simulating pulse-like ground motions. (1) The scheme is designed for acceleration ground motion simulation. However, the pulse usually exists in velocity ground motions. The

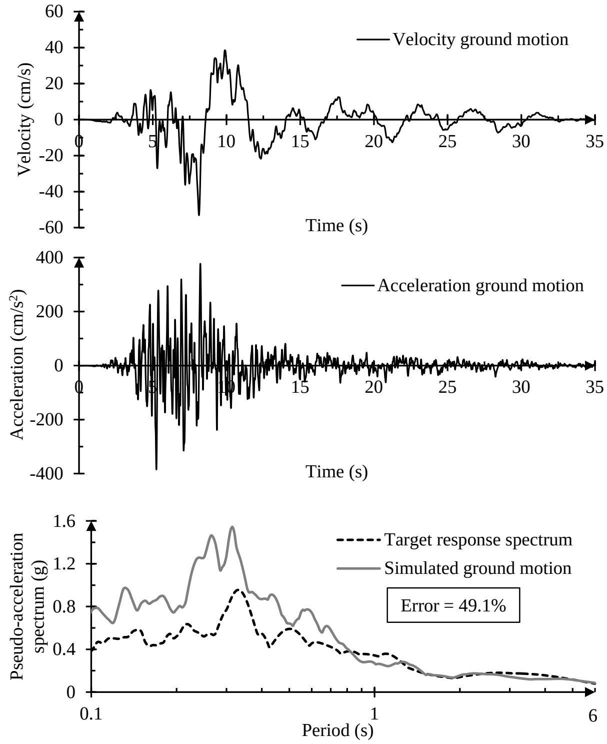

Figure 12: The simulated ground motion based on SRM.

pseudo-acceleration response spectrum cannot be applied to modify the PSDF of velocity ground motion. (2) The convergence of the iteration scheme is sensitive to the data size of the target response spectra. For example, the iteration scheme difficultly converges to the allowable error 10% when the data size of the target response spectra is 1200 that adopted in this study. In contrast, the proposed algorithm can effectively meet the requirement of spectrum compatibility in the same situation.

$$G_i^{(j+1)}(\omega) = G_i^{(j)}(\omega)\left[\frac{R_i^T(\omega)}{R_i^{(j)}(\omega)}\right] \tag{22}$$

where $R_i^T(\omega)$ is the target response spectrum; $R_i^{(j)}(\omega)$ and $G_i^{(j)}(\omega)$ is the pseudo-acceleration response spectrum and the PSDF of simulated ground motion at (j) iteration, respectively.

Shields's perturbation algorithm changes the PSDF randomly instead of using the rule shown in Eq. (22). The changed PSDF would be accepted if the changes made the spectral error less than the former iteration. Otherwise, the next iterations are performed and it would not terminate until satisfying the allowable error. Since the pseudo-acceleration response spectrum of simulated ground motion is not applied in this method, the PSDF of both velocity and acceleration ground motion can be effectively modified. Hence, Shields's algorithm is a potential way to solve the problem for SRM in simulating response spectrum compatible pulse-like ground motion. However, further studies are required to perform, such as keeping the pulse characteristic and the spectrum compatibility simultaneously.

The differences between Shields's algorithm and the proposed algorithm are briefly analyzed. Compared with the PSDF iteration in Shields's algorithm, the proposed algorithm directly modulates the ground motion in the time domain by adding the stochastic trigonometric series components. Besides, the amounts of random variables for each ground motion are specific in Shields's method when n in Eq. (19) is determined; however, the amounts of variables are uncertain in the proposed method since iteration items are variable. Finally, since different amplitude modulation functions are feasible for the proposed algorithm, both the pulse location and the shape of simulated pulse-like ground motions are variables. This property effectively ensures the diversity of simulated pulse-like ground motions.

6. Conclusions

Based on trigonometric series, this study proposes a novel stochastic method to mitigate the issue of the scarcity of pulse-like records, with advantages that the simulated pulse-like ground motion can satisfy the response spectrum requirement of artificial ground motion in anti-seismic codes, and be compatible with a given target spectrum. This method utilizes a Hilbert transform-based amplitude modulation function to ensure the simulated ground-motion velocity contains a pulse, and a random frequency parameter-based iteration scheme to make the pseudo-spectral acceleration of simulated ground motion compatible with the target spectrum. The effectiveness of the proposed method in enriching the existing pulse-like databases and generating artificial pulse-like ground motions in areas lacking records is verified by two cases.

The presence of pulse and the pulse period of simulated ground motion is controllable in the proposed method. Specifically, the amplitude modulation function determines the presence or absence of a pulse in the simulated ground motion velocity. Two workable amplitude modulation functions, the envelope function of pulse-like velocity obtained by Hilbert transform and the designed piecewise function, are proposed to guarantee the presence of a pulse. The maximum value of the amplitude modulation function also affects the convergence speed in spectrum compatibility analysis. According to the tests, the optimum maximum value of the amplitude modulation function ranges from 1/100 to 1/50 of target peak ground velocity. Besides, the pulse period of pulse-like ground motion mainly depends on the target spectrum. The ability that the simulated pulse-like ground motion is compatible with any target spectrum makes the method potentially universal applicability for stochastic pulse-like ground motion simulation in engineering.

Since the proposed method can effectively control the presence of a pulse and response spectrum, it may advance the seismic response analysis of near-fault pulse-like ground motion to better understand the impacts of the ground motion pulse and response spectrum on structural response. For example, the effects of the presence of a pulse on seismic response analysis can be analyzed on the condition of response spectrum compatibility using the ground motions generated by the same target spectrum but different amplitude modulation functions. It can also be utilized to evaluate the effects of the response spectrum of pulse-like ground motion on the seismic response using the ground motions generated by the same pulse-like envelope function but different target spectra.

Acknowledgements

This research is supported by the International Joint Research Platform Seed Fund Program of Wuhan University (Grant No. WHUZZJJ202207) and National Natural Science Foundation of China (Grant No. 52079099). Guan Chen would like to thank the financial support of Sino-German (CSC-DAAD) Postdoc Scholarship Program.

Conflict of interest

The authors declare that they have no known competing financial interests or personal relationships that could have appeared to influence the work reported in this paper.

References

[1] G. W. Housner, M. D. Trifunac, Analysis of accelerograms—Parkfield earthquake, Bulletin of the Seismological Society of America 57 (6) (1967) 1193–1220.

[2] K. Aki, Seismic displacements near a fault, Journal of Geophysical Research 73 (16) (1968) 5359–5376.

[3] E. Kalkan, S. K. Kunnath, Effects of fling step and forward directivity on seismic response of buildings, Earthquake Spectra 22 (2) (2006) 367–390.

[4] V. Phan, M. S. Saiidi, J. Anderson, H. Ghasemi, Near-fault ground motion effects on reinforced concrete bridge columns, Journal of Structural Engineering 133 (7) (2007) 982–989.

[5] A. Alonso-Rodríguez, E. Miranda, Assessment of building behavior under near-fault pulse-like ground motions through simplified models, Soil Dynamics and Earthquake Engineering 79 (2015) 47–58.

[6] L. Li, M. Fang, G. Chen, D. Yang, Reliability-based stochastic optimal control of frame building under near-fault ground motions, Mechanical Systems and Signal Processing 163 (2022) 108098.

[7] I. N. Psycharis, M. Fragiadakis, I. Stefanou, Seismic reliability assessment of classical columns subjected to near-fault ground motions, Earthquake Engineering & Structural Dynamics 42 (14) (2013) 2061–2079.

[8] G. P. Mavroeidis, A. S. Papageorgiou, A mathematical representation of near-fault ground motions, Bulletin of the Seismological Society of America 93 (3) (2003) 1099–1131.

[9] M. Dabaghi, A. Der Kiureghian, Stochastic model for simulation of near-fault ground motions, Earthquake Engineering & Structural Dynamics 46 (6) (2017) 963–984.

[10] P. Code, Eurocode 8: Design of structures for earthquake resistance-Part 1: General rules, seismic actions and rules for buildings, Brussels: European Committee for Standardization (2005).

[11] ASCE, Minimum design loads and associated criteria for buildings and other structures, ASCE standard ASCE/SEI 7-16. Reston, VA: American Society of Civil Engineers (2016).

[12] Y. Hisada, S. Tanaka, What is fling step? Its theory, simulation method, and applications to strong ground motion near surface fault ruptures, Bulletin of the Seismological Society of America 111 (5) (2021) 2486–2506.

[13] D. M. Boore, Simulation of ground motion using the stochastic method, Pure and Applied Geophysics 160 (3) (2003) 635–676.

[14] K.-Q. Li, D.-Q. Li, Y. Liu, Meso-scale investigations on the effective thermal conductivity of multi-phase materials using the finite element method, International Journal of Heat and Mass Transfer 151 (2020) 119383.

[15] S. Mukhopadhyay, V. K. Gupta, Directivity pulses in near-fault ground motions—I: Identification, extraction and modeling, Soil Dynamics and Earthquake Engineering 50 (2013) 1–15.

[16] L. S. Burks, J. W. Baker, A predictive model for fling-step in near-fault ground motions based on recordings and simulations, Soil Dynamics and Earthquake Engineering 80 (2016) 119–126.

[17] O. F. Yalcin, M. Dicleli, Effect of the high frequency components of near-fault ground motions on the response of linear and nonlinear SDOF systems: A moving average filtering approach, Soil Dynamics and Earthquake Engineering 129 (2020) 105922.

[18] S. Rezaeian, A. Der Kiureghian, A stochastic ground motion model with separable temporal and spectral nonstationarities, Earthquake Engineering & Structural Dynamics 37 (13) (2008) 1565–1584.

[19] M. Shinozuka, G. Deodatis, Stochastic process models for earthquake ground motion, Probabilistic Engineering Mechanics 3 (3) (1988) 114–123.

[20] B. W. Dickinson, H. P. Gavin, Parametric statistical generalization of uniform-hazard earthquake ground motions, Journal of Structural Engineering 137 (3) (2011) 410–422.

[21] J. W. Baker, Quantitative classification of near-fault ground motions using wavelet analysis, Bulletin of the Seismological Society of America 97 (5) (2007) 1486–1501.

[22] D. Yang, J. Zhou, A stochastic model and synthesis for near-fault impulsive ground motions, Earthquake Engineering & Structural Dynamics 44 (2) (2015) 243–264.

[23] G. G. Amiri, A. A. Rad, N. K. Hazaveh, Wavelet-based method for generating nonstationary artificial pulse-like near-fault ground motions, Computer-Aided Civil and Infrastructure Engineering 29 (10) (2014) 758–770.

[24] E. Zengin, N. A. Abrahamson, A procedure for matching the near-fault ground motions based on spectral accelerations and instantaneous power, Earthquake Spectra 37 (4) (2021) 2545–2561.

[25] X. Roman-Velez, L. A. Montejo, Generation of seed-based spectrum-compatible pulse-like time-series, Bulletin of Earthquake Engineering 18 (4) (2020) 1161–1186.

[26] G. Chen, Q. Y. Li, D. Q. Li, Z. Y. Wu, Y. Liu, Main frequency band of blast vibration signal based on wavelet packet transform, Applied Mathematical Modelling 74 (2019) 569–585.

[27] F. Naeim, A. Alimoradi, S. Pezeshk, Selection and scaling of ground motion time histories for structural design using genetic algorithms, Earthquake Spectra 20 (2) (2004) 413–426.

[28] G. Deodatis, Non-stationary stochastic vector processes: seismic ground motion applications, Probabilistic Engineering Mechanics 11 (3) (1996) 149–167.

[29] M. D. Shields, G. Deodatis, Estimation of evolutionary spectra for simulation of non-stationary and non-Gaussian stochastic processes, Computers & Structures 126 (2013) 149–163.

[30] A. Giaralis, P. D. Spanos, Wavelet-based response spectrum compatible synthesis of accelerograms—Eurocode application (EC8), Soil Dynamics and Earthquake Engineering 29 (1) (2009) 219–235.

[31] P. D. Spanos, I. A. Kougioumtzoglou, Harmonic wavelets based statistical linearization for response evolutionary power spectrum determination, Probabilistic Engineering Mechanics 27 (1) (2012) 57–68.

[32] P. D. Spanos, G. Failla, Evolutionary spectra estimation using wavelets, Journal of Engineering Mechanics 130 (8) (2004) 952–960.

[33] D. Huang, G. Wang, Energy-compatible and spectrum-compatible (ECSC) ground motion simulation using wavelet packets, Earthquake Engineering & Structural Dynamics 46 (11) (2017) 1855–1873.

[34] P. Cacciola, I. Zentner, Generation of response-spectrum-compatible artificial earthquake accelerograms with random joint time–frequency distributions, Probabilistic Engineering Mechanics 28 (2012) 52–58.

[35] M. D. Shields, Simulation of spatially correlated nonstationary response spectrum–compatible ground motion time histories, Journal of Engineering Mechanics 141 (6) (2015) 04014161.

[36] S. Mukherjee, V. K. Gupta, Wavelet-based generation of spectrum-compatible time-histories, Soil Dynamics and Earthquake Engineering 22 (9-12) (2002) 799–804.

[37] Y. Li, G. Wang, Simulation and generation of spectrum-compatible ground motions based on wavelet packet method, Soil Dynamics and Earthquake Engineering 87 (2016) 44–51.

[38] D. Cecini, A. Palmeri, Spectrum-compatible accelerograms with harmonic wavelets, Computers & Structures 147 (2015) 26–35.

[39] Z. Dai, X. Li, C. Hou, An optimization method for the generation of ground motions compatible with multi-damping design spectra, Soil Dynamics and Earthquake Engineering 66 (2014) 199–205.

[40] F. Zhao, Y. Zhang, H. Lü, Artificial ground motion compatible with specified ground shaking peaks and target response spectrum, Earthquake Engineering and Engineering Vibration 5 (1) (2006) 41–48.

[41] M. Shinozuka, G. Deodatis, Simulation of stochastic processes by spectral representation, Applied Mechanics Reviews 44 (4) (1991) 191–204.

[42] M. Grigoriu, Simulation of nonstationary Gaussian processes by random trigonometric polynomials, Journal of Engineering Mechanics 119 (2) (1993a) 328–343.

[43] H. Hao, Effects of spatial variation of ground motions on large multiply-supported structures, Report No. UCB/EERC-89/06 of University of California Berkeley (1989).

[44] M. Le Van Quyen, J. Foucher, J. P. Lachaux, E. Rodriguez, A. Lutz, J. Martinerie, F. J. Varela, Comparison of Hilbert transform and wavelet methods for the analysis of neuronal synchrony, Journal of Neuroscience Methods 111 (2) (2001) 83–98.

[45] M. Feldman, Hilbert transform in vibration analysis, Mechanical Systems and Signal Processing 25 (3) (2011) 735–802.

[46] G. Chen, M. Beer, Y. Liu, Identification of near-fault multi-pulse ground motion Under review (2022).

[47] G. Chen, K. Li, Y. Liu, Applicability of continuous, stationary, and discrete wavelet transforms in engineering signal processing, Journal of Performance of Constructed Facilities 35 (5) (2021) 04021060.

[48] P. C. Jennings, G. W. Housner, N. C. Tsai, Simulated earthquake motions, Report of California Institute of Technology (1968).

[49] M. Shinozuka, Y. Sato, Simulation of nonstationary random process, Journal of the Engineering Mechanics Division 93 (1) (1967) 11–40.

[50] M. Shinozuka, Monte carlo solution of structural dynamics, Computers & Structures 2 (5-6) (1972) 855–874.

[51] M. Shinozuka, C. M. Jan, Digital simulation of random processes and its applications, Journal of Sound and Vibration 25 (1) (1972) 111–128.

[52] M. Grigoriu, On the spectral representation method in simulation, Probabilistic Engineering Mechanics 8 (2) (1993b) 75–90.